

The Astrophysical Behavior of Open Clusters along the Milky Way Galaxy

Tadross, A. L.

National Research Institute of Astronomy and Geophysics, 11421 - Helwan, Cairo, Egypt.

altadross@yahoo.com

ABSTRACT

The main aim of this paper is to study the astrophysical behaviour of open clusters' properties along the Milky Way Galaxy. Near-IR JHK_S ($2MASS$) photometry has been used for getting a homogeneous Catalog of 263 open clusters' parameters, which are randomly selected and studied by the author through the last five years; most of them were studied for the first time. The correlations between the astrophysical parameters of these clusters have been achieved by morphological way and compared with the most recent works.

Subject headings: Galaxy: open clusters and associations – astrometry – Stars – astronomical databases: catalogs.

1. Introduction

Open star clusters are very important objects in solving problems of star formation, stellar evolution, and improving our knowledge about the distance scale and the kinematic properties of the Milky Way Galaxy. This kind of study requires a large set of homogeneous data on the positions and ages of open star clusters, which are estimated in a precision way from their Colour-Magnitude Diagrams (*CMDs*). However, it is useful to re-investigate the properties and structures of the Milky Way Galaxy using the most recent Near-IR JHK_S photometric data from the 2-Micron All Sky Survey ($2MASS$) Point Source Catalogue of Skrutskie et al. (2006). In this context, we used a sample of 263 open star clusters (most of them are studied for the first time) that have been analysed by the author, in a series of papers; Tadross (2008 ~ 2012); see Tables 1 and 2. Our aim is to repeat the work we have done 12 years ago, Tadross 2001 and Tadross et al. 2002, to study such relations using NIR observations instead of UBV.

This paper is organized as follows. In Sec. 2, a historical review of the present study is obtained. In Sec. 3, data analysis of the clusters under investigation are presented. The

limiting and core radii are given in Sec. 4. The main photometric parameters are obtained in Sec. 5. Ages and locations, distribution are presented in Sec. 6. Reddening distribution is presented in Sec. 7. The diameters and ages' relations are given in Secs. 8 and 9 respectively. Secs. 10 and 11 describe the spiral arms and warp of the Galaxy respectively. The conclusions are obtained in Sec. 12.

2. Historical Review

Recently, Bukowiecki et al. (2011) determined new coordinates of the centres, angular sizes and radial density profiles for 849 open clusters in the Galaxy based on the *2MASS* database. Froebrich et al. (2010) studied 269 open clusters; ages, core radii, reddening, Galactocentric distances and the scale-heights were determined. Similar to this kind of study, Schilbach et al. (2006) derived the linear sizes of some 600 clusters and investigated the effect of the mass segregation of stars in open clusters. Bica et al. (2003) researched 346 open clusters, based on the *2MASS* database; they studied the linear diameters and spatial distribution of open clusters in the Galaxy. Tadross (2001) and Tadross et al. (2002) studied 160 open clusters used *UBV-CCD* observations and derived the relationships projected onto the Galactic plane in morphological way. Dutra & Bica (2001) studied 42 new infrared star clusters, stellar groups and candidates towards the Cygnus X region. Dutra & Bica (2000) have studied 103 Galactic open clusters and compared the reddening values obtained from far infrared *IRAS* and *COBE* observations with those obtained from visible observations. Dambis (1999) determined the main parameters of 203 open clusters based on the published photoelectric and CCD data. Malyshева (1997) published a Catalogue of parameters for 73 open clusters determined from $uvby\beta$ photometry; his values are in good agreement with those of Loktin & Matkin (1994). Loktin et al. (1997) published his improved version Catalogue, which contained the updated parameters of homogeneously estimated excesses, distances, and ages for 367 open clusters. Friel (1995) and Janes & Phelps (1994) based on a sample of some 70 objects investigated how the extinction and age depend on the position in the Galaxy. Also, a comparison between the age and position in the Galaxy was studied by Lyngå (1980, 1982). In addition an old study of Janes (1979) used *UBV* photometry to study the reddening and metallicity of 41 open clusters.

3. Data analysis

The current study depended mainly on the correlations between the astrophysical parameters of 263 open star clusters of different names listed as follows: 124 clusters of NGC;

24 objects of Berkeley; 23 of Kronberger; 23 of Czernik; 11 of Dol-Dzim; 11 of Ruprecht; 10 of Dolidze; 6 of Dias; 5 of Turner; 4 of King; 3 of BH; 3 of Eso; 3 of IC; 2 of Alessi; 2 of Juchert; 2 of Riddle; 2 of Skiff; 2 of Teutsch; 1 of Collinder; 1 of Patchick; and 1 cluster of Toepler.

This sample contains clusters with ages in the range from 5 Myr to 5 Gyr. They are located at distances up to 4.7 kpc from the Sun (R_\odot), up to 12.5 kpc from the Galactic Centre (R_{gc}), and less than ± 2 kpc from the Galactic Plane (Z). They range from 0.25 to 16.5 arcmin in limiting radii ($R_{lim.}$), and up to 1 arcmin in core radii (R_c); with noticing that the estimated $R_{lim.}$ and R_c in parsecs depending mainly on the distance of the clusters individually.

Data extraction has been performed for each cluster using the known tool of VizieR for 2MASS¹ Point Source Catalogue database of Skrutskie et al. (2006). The investigated clusters have been selected from WEBDA and DIAS databases under some conditions mentioned in our last series papers. It is noticed that most clusters' sizes seem to be greater in the infrared band (2MASS observations) than in the optical band; because this system can detect the very faint stars, even those behind the curtains of interstellar matter. The real spatial distribution of open clusters along the Milky Way Galaxy refers to some paucity of the clusters at G. longitudes range from 140° to 200°. The lack of objects in that direction is noticed also in earlier studies and confirmed for open clusters by Benjamin (2008), and Bukowiecki et al. (2011). Older clusters seem to be more dispersed than younger ones of the Hyades, as shown in the left panel of Fig. 1. The relationships between the astrophysical parameters of open clusters are presented here with respect to their ages and places, so then the astrophysical behaviour of open clusters along the Milky Way Galaxy can be investigated.

4. Limiting and core radii

One of the main tasks in this work was the determination of the radial density profile (RDP) for each cluster, i.e. the observed stellar density ρ that plotted as a function of the angular radial distance from the cluster centre, King (1966):

$$\rho(r) = f_{bg} + \frac{f_0}{1+(R_{lim}/R_c)^2}$$

where R_c , f_0 , and f_{bg} are the core radius, the central density, and the background density, respectively. The core radius was derived as a distance where the stellar density drops

¹<http://vizier.u-strasbg.fr/viz-bin/VizieR?-source=2MASS>

to half of f_0 . The parameters were derived with the least-square method. The cluster's limiting radius, R_{lim} , was defined by comparing $\rho(r)$ with the background density level ρ_{bg} , (cf. Bukowiecki et al. 2011). From both R_c and R_{lim} , one can estimate the concentration parameter $c = \log(R_{lim}/R_c)$, Peterson & King (1975). This parameter can be added as a new item to characterise the structure of clusters along the Galaxy. In the present work, the concentration parameters are ranging from 0.39 to 2.5. In this context, Nilakshi et al. (2002) concluded that the angular size of the coronal region is about 6 times the core radius, while Maciejewski & Niedzielski (2007) reported that R_{lim} may vary for individual clusters from $2R_c$ to $7R_c$. In our case, for the whole sample, the average values of limiting radius, core radius, and concentration parameter are 4.6 arcmin, 0.3 arcmin, and 1.2 respectively. We concluded that $R_{lim} = 6.85 R_c$; for the clusters up to $R_c = 0.5$ arcmin, and $R_{lim} = 2.88 R_c$; for the clusters up to $R_c = 1.0$ arcmin. i.e, our conclusion is almost in agreement with Maciejewski & Niedzielski (2007).

5. Main photometric parameters

Depending on the 2MASS data, deep stellar analyses of the candidate clusters have been presented. The photometric data of 2MASS not only allow us to construct of relatively well defined CM diagrams of the clusters, but also permit a more reliable determination of astrophysical parameters. In this paper, we used extraction areas having a radius of 20 arcmin, which are larger than the estimated limiting radius of the clusters. Because of the weak contrast between the cluster and the background field density, some inaccurate statistical results may be produced beyond the real limit of cluster borders (Tadross, 2005).

The main astrophysical parameters of the clusters, e.g. age, reddening, distance modulus, can be determined by fitting the isochrones to the cluster CMDs. To do this, we applied several fittings on the CMDs of the clusters by using the stellar evolution models of Marigo et al. (2008) of Padova isochrones on the solar metallicity. It is worth mentioning that the assumptions of solar metallicity are quite adequate for young and intermediate age open clusters, which are closer to the Galactic disk. So, Near-Infrared surveys are very useful for the investigation of such clusters. It is relatively less affected by high reddening from the Galactic plane. However, for a specific age isochrones, the fit should be obtained at the same distance modulus for both diagrams [$J-(J-H)$ & $K_s-(J-K_s)$], and the color excesses should obey Fiorucci & Munari (2003)'s relations for normal interstellar medium. We note that, it is difficult to obtain some accurate determinations of the astrophysical parameters due to the weak contrast between clusters and field stars.

Reddening determination is one of the major steps in the cluster compilation. Therefore,

it estimated guiding by Schlegel et al. (1998) in our estimations. In this context, for color excesses transformations, we used the coefficient ratios $\frac{A_J}{A_V} = 0.276$ and $\frac{A_H}{A_V} = 0.176$, which were derived from absorption ratios in Schlegel et al. (1998), while the ratio $\frac{A_{Ks}}{A_V} = 0.118$ was derived from Dutra et al. (2002). Applying the calculations of Fiorucci & Munari (2003) for the color excess of 2MASS photometric system; we ended up with the following results: $\frac{E_{J-H}}{E_{B-V}} = 0.309 \pm 0.130$, $\frac{E_{J-Ks}}{E_{B-V}} = 0.485 \pm 0.150$, where $R_V = \frac{A_V}{E_{B-V}} = 3.1$. Also, we can de-reddened the distance modulus using these formulae: $\frac{A_J}{E_{B-V}} = 0.887$, $\frac{A_{Ks}}{E_{B-V}} = 0.322$. Then the distance of each cluster from the Sun, R_\odot , can be calculated. Consequently, the distance from the Galactic plane (Z_\odot), and the projected distances in the Galactic plane from the Sun (X_\odot & Y_\odot) can be determined, see Table 3. For more details about the distance calculations, see Tadross (2011).

6. Ages and locations

The distribution of our sample according the distances from the Galactic center, R_{gc} , and the height from the Galactic plane, Z , is presented in the right panel of Fig. 1. We can see that the clusters with ages younger than Hyades, i.e. less than $(7 \times 10^8 \text{ yr})$ are strongly concentrated to the Galactic plane. While the clusters which are older than Hyades are more dispersed from the Galactic plane (cf. Friel 1995). However, the correlations of the clusters' ages and locations with the other properties along the Milky Way Galaxy are presented in the following sections.

7. Reddening distribution

In fact reddening affects the distance determination via the main sequence fitting, actually it affected all the cluster's dimensions and positions on the Galaxy (cf. Tadross et al. 2002). The distribution of the reddening of our sample versus the Galactic latitudes confirms that the higher values of reddening are concentrated on and near the Galactic plane as shown in Fig. 2. Along the Galactic longitude bins of 20° the distribution of the mean reddening at each bin show that the higher values are concentrated around the longitude range from 345° to 130° , i.e. in the directions of the Galactic centre and Sagittarius arm, as shown in Fig. 3. The general trend of reddening with age shows that reddening decreases with ages where younger clusters tend to be more reddened than older ones, see Fig. 4. On the other hand, the relation between reddening and R_{gc} reveals that the clusters inside the galactocentric radius of the Sun ($R_{gc\odot} = 8.5 \text{ kpc}$) have higher values of reddening than that of outside ones, as shown in Fig. 5. This confirms to some extent that the Sun's vicinity

clusters are young and medium ones than those outside clusters.

8. Diameters' relations

The linear diameters have been plotted versus the absolute values of the height from the Galactic plane $|Z|$, and the distance from the Galactic centre R_{gc} as shown in Fig. 6 and Fig. 7 respectively. We can see that most clusters with typical diameters ($D < 10$ pc) are concentrated near the Galactic plane, especially those inside the galactocentric radius of the Sun $R_{gc} \leq 8.5$ kpc. The general trend of this relation appears that large, old clusters are found far from R_{gc} - it is confirmed by Bukowiecki et al. (2011)- and also at large height Z (Tadross et al. 2002). There are some young clusters with larger diameters belong to the Galactic plane are loose and unbound objects. The relation between the diameters and the galactocentric radii has been examined to be:

$$\text{Diam.} = 0.53 R_{gc} - 0.19$$

The standard error of this relation ≈ 3.0

Burki and Maeder (1976) found a correlation between these quantities only for the very young clusters, but we have found such correlation for intermediate and older clusters as well.

Fig. 8 represents the relation between ages and linear diameters of our sample. It can be expressed as follows:

$$\text{Diam.} = 3.18 \log(\text{age}) - 18.53$$

The standard error of this relation ≈ 3.2

We can see that, to some extent, there is a correlation between diameters and ages, whereas clusters of large sizes belong to older ages, which have also large heights from Z . Youngest clusters with large sizes are supposed to be some groups of OB associations and probably they are not bound systems (Lyngå 1982; Janes, Tilley & Lyngå 1988). Massive clusters with small sizes will be dissolved due to encounters among their members, while those of very large sizes with the same mass will be unstable in the Galactic tidal field, and they may take very long time to have stability and relaxation (Theis 2001). Small clusters with typical diameters less than 10 pc show a concentration to the Galactic plane (Wielen 1971 and 1975) in the range of $|Z| < 100$ pc, see Fig. 6, but larger clusters have both intermediate and old ages.

9. Ages' relations

The cluster's ages has been plotted versus Z , as shown in Fig. 9. Most clusters with ages $t \leq 10^{8.9}$ yr is lying around $|Z| \approx 200$ PC, while older ones are lying higher than such heights. It indicated that the thickness of the Galactic disk has not changed on the time scale of about $10^{9.0}$ yr and the clusters can be formed everywhere inside this layer (cf. Tadross et al. 2002). Lyngå & Palous (1987) have found that old clusters are much thicker distributed in the outer parts of the Galaxy than the inner parts, Bukowiecki et al. (2011). Also in our study the thickness of the Galactic disk increases for older clusters as well. Old clusters not only spend their time in the outer disk away from the disruptive effects of giant molecular clouds, but also, they spend their time at large distances from the Galactic plane, further enhancing their survivability (Friel 1995).

On the other hand, the relation between ages and R_{gc} of the clusters implies that there is a lack of old clusters in the inner parts of the Galactic disk, and the anti-center clusters survive longer than such clusters. In the inner parts of the Galaxy they have never gotten the relaxation state in the fluctuating gravitational field of that part (Lyngå, 1980; McClure et al., 1981; Vanden Bergh, 1985). The general trend reveals that, lifetime increases outwards the Milky Way Galaxy, where clusters live longer than those in the inner parts of it.

10. Galactic spiral arms

To show the shape of the spiral arms of the Galaxy, several studies have been carried out in the last five decades. The positions of the clusters on the Galactic plane have been used to trace the spiral arms of the Milky Way Galaxy. Centered on the Sun at ($X_\odot = Y_\odot = 0$) the distribution of the clusters on the Galactic plane has been plotted, as shown in Fig. 10. Within a radius of 4 kpc from the sun (cf. Jeanes, Tilley & Lyngå 1988) the distribution of the studied clusters define three concentration features which are related to the spiral structure of the Galaxy, i.e. Perseus, Sagittarius and Carina. It is assumed that there are more than three arms of the Galaxy but because of the patchy cloud and absorption effects we can't able to detect them all!.

11. Galactic warp

The effect of the Galactic warp may be declared from the distribution of the open clusters of our sample using the Galactic coordinates X and Y versus the height Z within ± 2 kpc from the Galactic plane, as shown in Fig. 11. The directions of the G. X and G. Y

defined to be positive in the direction of the Galactic radial center and towards the direction of Galactic rotation respectively (Jeanes, Tilley & Lyngå 1988; Camerón 1999; Piatti et al. 2003). No strong indication to the warp has been detected on the G. X direction, but, to some extent, it can be detected on the G. Y direction. This may refer to the leak of the studied clusters, especially those have large distances from the sun’s vicinity (Tadross et al. 2002).

12. Conclusion

The results of our studied clusters in the last five years using near-infrared JHK_S photometric system are obtained here, and the correlations between the astrophysical parameters along the Milky Way Galaxy are achieved. It is obvious that (JHK_S) 2MASS system affected the magnitude limit of the clusters, which detects many faint members located away from the cluster’s core, so then the cluster seems to be larger than in optical bands. Detecting stars located in the lower parts of CMDs, make the fitting with standard zero age main sequence much easier. This, of course, has contributed to the evaluation of the cluster parameters, i.e. distances, diameters, ages, reddening, etc. From our reduction, we concluded that $R_{lim} = 6.85 R_c$; for the clusters up to $R_c = 0.5$ arcmin, and $R_{lim} = 2.88 R_c$; for the clusters up to $R_c = 1.0$ arcmin, which are in agreement with Maciejewski & Niedzielski (2007). We also noticed that the linear size of open clusters increases with ages. The reddening decreases outward the Galactic plane, Z and the Galactic Center, R_{gc} , as well. This is noticed also for clusters located near the Sun vicinity and further than 8.5 kpc from the Galactic centre, i.e. the density of dust and gas decreases, too.

From our analysis, we noticed that the number of clusters decreases with Z ; more than half of the studied clusters (52%) have aged less than 500 mega years and located at average $|Z| = 75$ pc. Hence, the older ones are located at average $|Z| = 275$ pc, which is in agreement with Bukowiecki et al. (2011). We can show that the difference between younger and older clusters can be declared in locations and sizes as the following relation:

$$\text{Diam.} = 0.53 R_{gc} - 0.19 = 3.18 \log(\text{age}) - 18.53$$

We found that the number of older clusters increases with R_{gc} and younger ones are obtained at an average $R_{gc} = 8.8$ kpc, which is confirmed by Tadross et al. (2002), Froebrich (2010), and Bukowiecki et al. (2011). The paucity of the clusters at G. longitudes range from 140° to 200° is noticeable by Tadross et al. (2002), Benjamin (2008), Froebrich (2010), and Bukowiecki et al. (2011). It may reflect the real spatial structure of the Milky Way Galaxy

in that direction near the feature region of the Perseus arm (the external youngest arm of the Galaxy).

This publication makes use of data products from the Naval Observatory Merged Astrometric Dataset (*NOMAD*) and the Two Micron All Sky Survey *2MASS*, which is a joint project of the University of Massachusetts and the Infrared Processing and Analysis Centre/California Institute of Technology, funded by the National Aeronautics and Space Administration and the National Science Foundation. Catalogues from *CDS/SIMBAD* (Strasbourg), and Digitized Sky Survey *DSS* images from the Space Telescope Science Institute have been employed.

REFERENCES

- Benjamin, R. A., 2008, BAAS, 40, 266
- Bica, E., Bonatto, Ch., Dutra, C.M., 2003, A&A, 405, 991
- Bukowiecki, L. et al., 2011, Acta Astronomica, 61, 231
- Burki G., Maeder A., 1976, A&A,, 51, 247
- Camerón, F., 1999, A&A, 351, 506
- Dambis, A. K., 1999, Astronomy Letters, 25, 7
- Dutra, C., Bica, E., 2000, A&A, 359, 347
- Dutra, C., Bica, E., 2001, A&A, 376, 434
- Dutra, C. et al., 2002, A&A, 381, 219
- Fiorucci, M., Munari, U., 2003, A&A, 401, 781
- Friel, E. D., 1995, Annu. Rev. Astron. Astrophys., 33, 381
- Froebrich, D. et al., 2010, MNRAS, 409, 1281
- Janes, K. A., 1979, Astrophys. J. Suppl., 39, 135
- Janes, K., Tilley, C., Lyngå, G., 1988, Astron. J., 95, 771
- Janes, K. A., Phelps, R. L., 1994, AJ, 108, 1773
- King, I., 1966, AJ, 71, 64
- Loktin, A.V., Matkin, N., 1994, Astron. Astrophys. Trans., 4, 153
- Loktin, A.V. et al., 1997, Baltic Astronomy, 6, 316
- Lyngå, G., 1980, IAU symposium, 85, 13 [ed. by J.E. Hesser (Reidel, Dordrecht)]
- Lyngå, G., 1982, Astro. Astrophys., 109, 213
- Lyngå, G., Palous, J., 1987, Astro. Astrophys., 188, 35
- Maciejewski, G., Niedzielski, A., 2007, A&A, 467, 1065
- Malysheva, L., 1997, Astron. Letters, 23, 585

- Marigo, P., et al. 2008, A&A, 482, 883
- McClure, R. et al., 1981, Astrophys. J., 243, 841
- Nilakshi, S. R. et al., 2002, A&A, 383, 153
- Peterson, C. J., King, I. R., 1975, AJ, 80, 427
- Piatti, A. et al., 2003, MNRAS, 346, 390
- Schilbach, E. et al., 2006, A&A, 456, 523
- Schlegel, D. et al. 1998, ApJ, 500, 525
- Skrutskie, M., et al., 2006, AJ, 131, 1163
- Tadross, A. L., 2001, New Astronomy, 6, no. 5, 293
- Tadross, A. L. et al., 2002, New Astronomy, 7, 553
- Tadross, A. L. 2005, AN, 326, 19
- Tadross, A. L., 2008a, New A, 13, 370
- Tadross, A. L., 2008b, MNRAS, 389, 285
- Tadross, A. L., 2009a, New A, 14, 2000
- Tadross, A. L., 2009b, Astrophys & Space Sci. 323, 383
- Tadross, A. L., Nasser, M. A., 2010, NRIAG Journal Ser."A67" (arXiv:1011.2934)
- Tadross, A. L., 2011, JKAS, 44 (1), 1
- Tadross, A. L., et al, 2012, RAA, 12, 75
- Tadross, A. L., 2012a, RAA, 12, 158
- Tadross, A. L., 2012b, New A, 17, 198
- Theis, Ch. 2001, Astronomische Gesellschaft Abs. Ser., 18, Annual Scientific Meeting JE-NAM 2001 # MS 05 47
- Vanden Bergh, D., 1985, Astrophys. Suppl., 58, 711
- Wielen, R. 1971, A&A, 13, 309

Wielen, R. 1975, IAU symposium, 69, 119 [ed. by A. Hayli (Reidel, Dordrecht)]

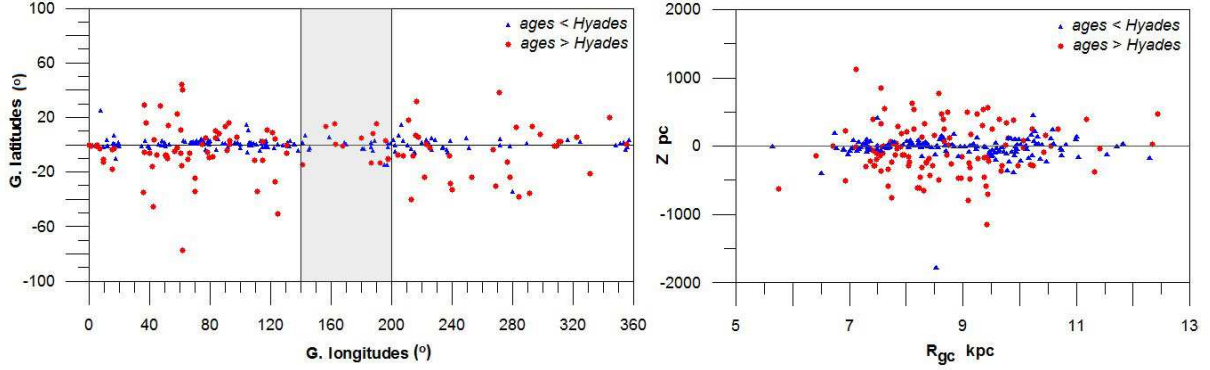


Fig. 1.— Left panel represents the clusters' distribution according to their Galactic longitudes and latitudes, the dark area refers to the paucity of the clusters at G. longitudes range from 140° to 200° . Right panel represents the clusters' distribution according their distances from the Galactic centre, R_{gc} , and Galactic plane, Z , assuming that $Z_\odot = -33$ pc, and $R_{gc\odot} = 8.5$ kpc for the Sun. Both panels plotted for two ranges of clusters' ages, younger and older than Hyades.

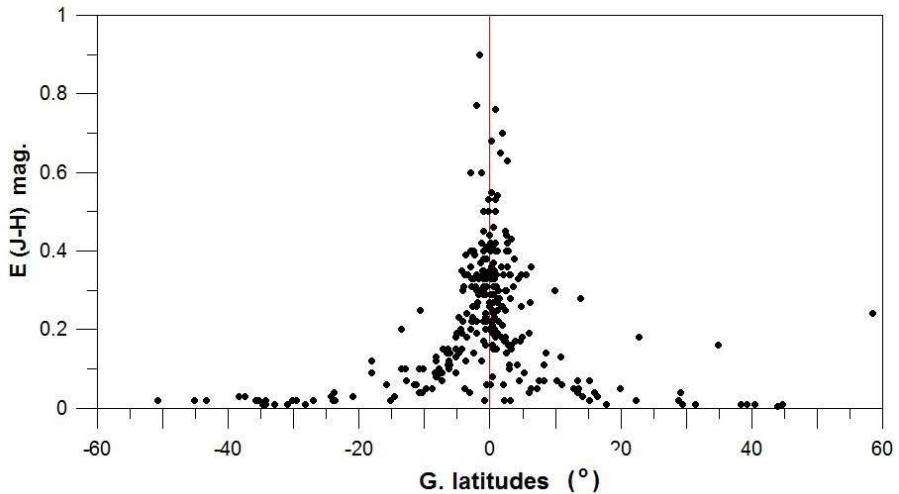


Fig. 2.— The distribution of the reddening versus the Galactic latitudes.

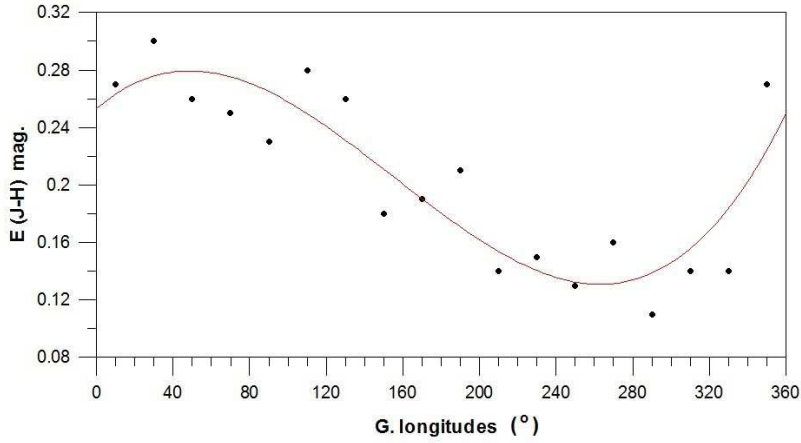


Fig. 3.— The distribution of the mean reddening along the Galactic longitude bins of 20 degrees for each.

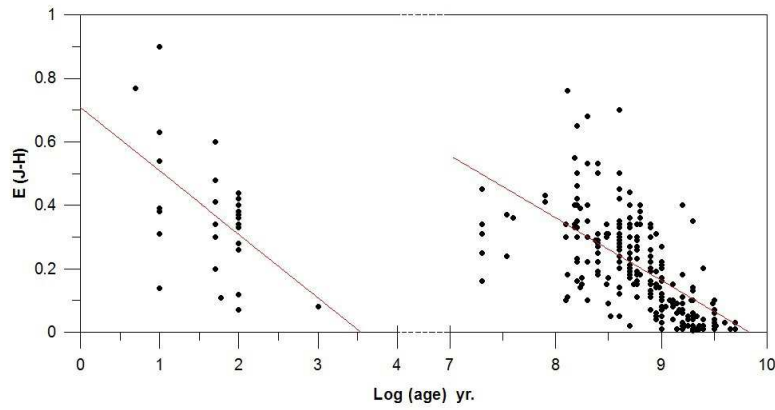


Fig. 4.— The relation between the clusters' ages and reddening. Left and right panels represent the very young and old clusters respectively.

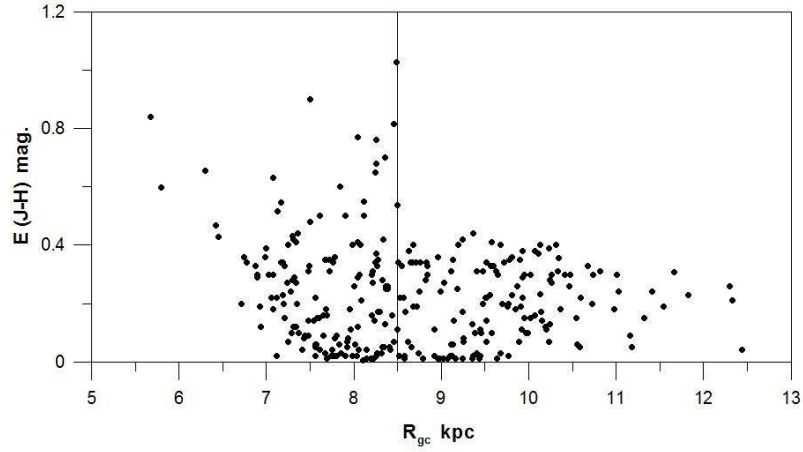


Fig. 5.— The relation between the reddening and distance from the Galactic centre R_{gc} . The vertical line represents the galactocentric radius of the Sun, assuming that $R_{gc\odot} = 8.5$ kpc.

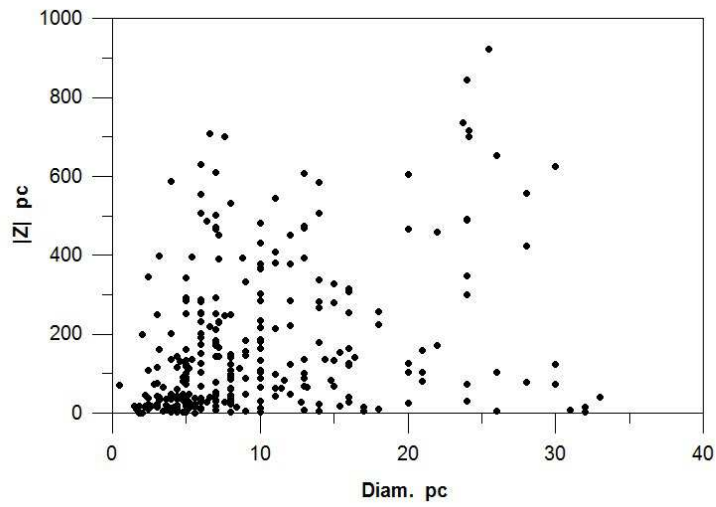


Fig. 6.— The relation between the diameters and the absolute values of the height from the Galactic plane, $|Z|$.

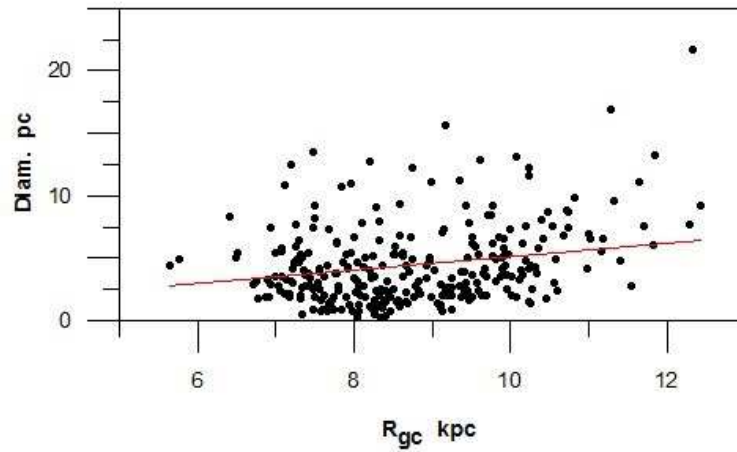


Fig. 7.— The relation between the galactocentric radii, R_{gc} , and linear diameters of the clusters, assuming that $R_{gc\odot} = 8.5$ kpc for the Sun. The standard error ≈ 3.0

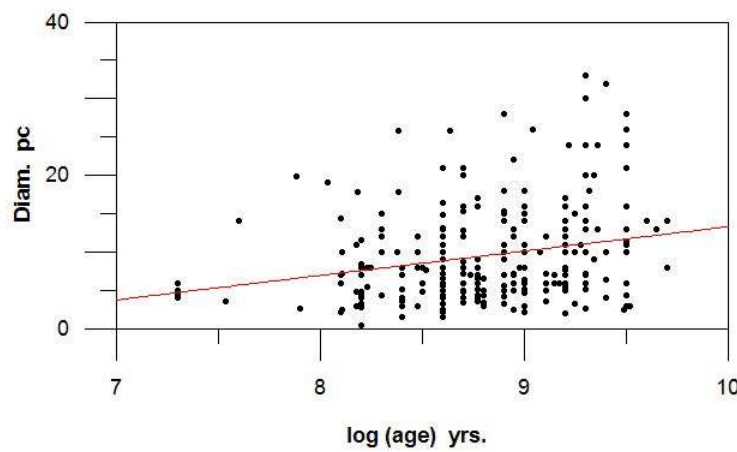


Fig. 8.— The relation between ages and linear diameters of the studied clusters. The standard error ≈ 3.2 .

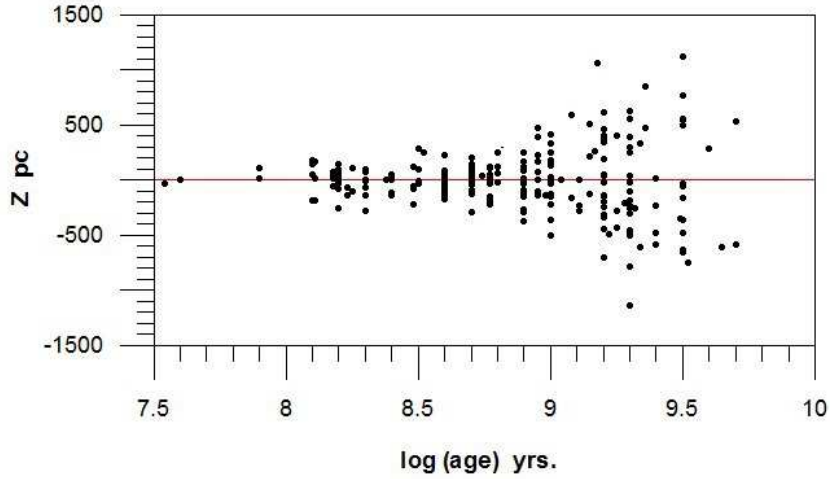


Fig. 9.— The relation between ages and the heights from the Galactic plane, assuming that $Z_{\odot} = -33$ pc for the Sun.

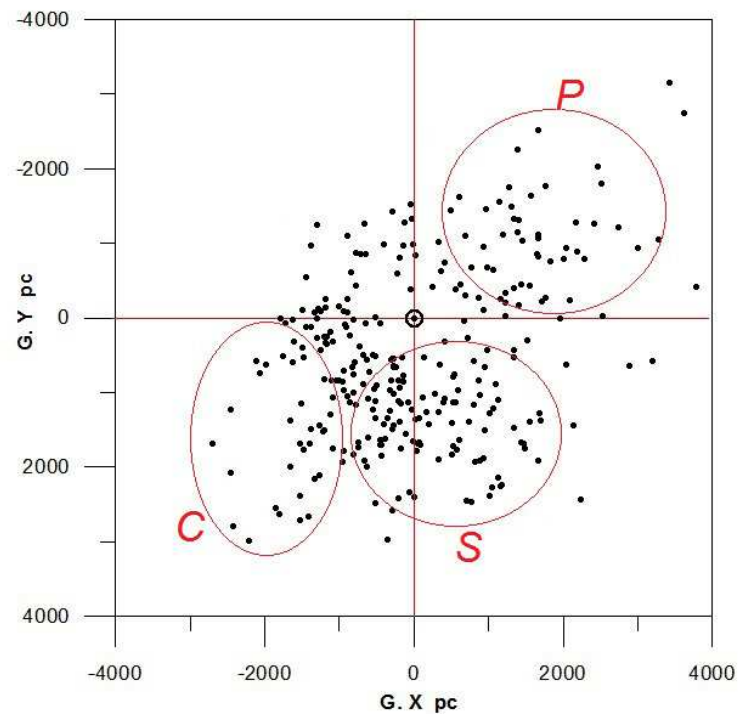


Fig. 10.— The distribution of our sample on the Galactic plane. The three circles refer to the three famous arms of the Galaxy: Perseus (P), Sagittarius (S), and Carina (C).

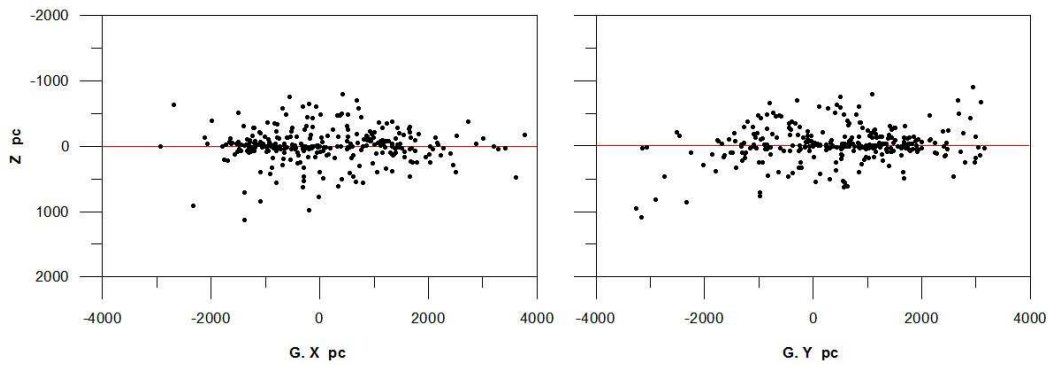


Fig. 11.— The distribution of our sample according to their Galactic coordinates X_{\odot} and Y_{\odot} versus the height from the Galactic plane Z . The Sun's position is at $X_{\odot} = Y_{\odot} = 0$.

Table 1: The astrophysical main parameters for the studied clusters, derived by the author. Columns display, respectively, cluster name, equatorial positions, angular limiting radius, core radius, age, reddening, distance from the sun R_{\odot} , distance from the Galactic centre R_{gc} , the projected distances on the Galactic plane from the sun X_{\odot} , Y_{\odot} , Z , and the reference for each cluster.

Cluster	α	δ	$R_{lim.}$	R_c	Age	E_{B-V}	R_{\odot}	R_{gc}	X_{\odot}	Y_{\odot}	Z	Ref.				
	h	m	s	$^{\circ}$	$'$	$''$	$'$	$'$	pc	kpc	pc	pc				
NGC 110	00	27	25	71	23	00	11.0	0.60	$0.9^{+0.04}$	$0.46^{+0.10}$	1150^{+53}	9.14	585	975	172	6
NGC 272	00	51	24	35	49	54	3.2	0.29	$2.5^{+0.10}$	$0.06^{+0.02}$	1068^{+50}	9.12	517	798	-486	6
NGC 657	01	43	21	55	50	11	3.0	0.90	$1.6^{+0.11}$	$0.34^{+0.05}$	1372^{+63}	9.44	881	1041	-151	6
NGC 743	01	58	37	60	09	18	4.0	0.26	$0.5^{+0.02}$	$0.95^{+0.20}$	1618^{+75}	9.64	1065	1217	-46	6
NGC 956	02	32	30	44	35	36	5.0	0.64	$1.0^{+0.04}$	$0.10^{+0.05}$	1455^{+67}	9.68	1097	883	-367	6
NGC 1498	04	00	18	-12	00	54	3.8	0.68	$1.6^{+0.11}$	$0.04^{+0.02}$	1020^{+47}	9.44	680	-297	-700	6
NGC 1520	03	57	51	-76	47	42	3.6	0.50	$2.0^{+0.08}$	$0.06^{+0.01}$	775^{+36}	8.25	-227	-587	-452	6
NGC 1557	04	13	11	-70	28	18	13.0	0.10	$3.0^{+0.12}$	$0.11^{+0.05}$	1055^{+49}	8.31	-197	-805	-653	6
NGC 1724	05	03	32	49	29	30	8.0	0.80	$0.6^{+0.02}$	$0.57^{+0.10}$	1437^{+66}	9.85	1332	526	121	6
NGC 1785	04	58	35	-68	50	40	3.0	0.25	$0.5^{+0.02}$	$0.06^{+0.02}$	3080^{+140}	8.52	-437	-2477	-1777	6
NGC 1807	05	10	43	16	31	18	9.0	0.46	$1.0^{+0.04}$	$0.32^{+0.05}$	960^{+44}	9.46	928	-99	-224	6
NGC 1857	05	20	12	39	21	00	4.0	0.08	$0.16^{+0.12}$	$0.97^{+0.20}$	1545^{+71}	10.02	1513	310	34	6
NGC 1891	05	21	25	-35	44	24	10.0	0.14	$2.0^{+0.05}$	$0.03^{+0.02}$	860^{+40}	8.96	364	-624	-467	6
NGC 2013	05	44	01	55	47	36	3.0	0.32	$1.5^{+0.06}$	$0.23^{+0.05}$	1100^{+51}	9.52	981	426	255	6
NGC 2017	05	39	17	-17	50	48	6.0	0.69	$1.6^{+0.11}$	$0.06^{+0.02}$	1120^{+52}	9.37	767	-681	-450	6
NGC 2026	05	43	12	20	08	00	8.0	0.38	$0.55^{+0.02}$	$0.60^{+0.10}$	1418^{+65}	9.91	1401	-178	-125	6
NGC 2039	05	44	00	08	41	30	5.0	0.36	$1.2^{+0.05}$	$0.32^{+0.05}$	920^{+42}	9.38	863	-273	-164	6
NGC 2061	05	42	42	-34	00	34	9.0	0.96	$2.1^{+0.08}$	$0.03^{+0.01}$	542^{+25}	8.79	246	-409	-256	6
NGC 2063	05	46	43	08	46	54	6.0	0.80	$1.3^{+0.05}$	$0.32^{+0.05}$	1525^{+70}	9.97	1430	-445	-285	6
NGC 2132	05	55	18	-59	54	36	12.0	0.38	$1.65^{+0.12}$	$0.06^{+0.02}$	974^{+45}	8.58	19	-842	-490	6
NGC 2165	06	11	04	51	40	36	5.0	0.44	$1.5^{+0.06}$	$0.23^{+0.05}$	1445^{+67}	9.89	1328	427	377	6
NGC 2189	06	12	09	01	03	54	7.0	0.78	$0.8^{+0.03}$	$0.39^{+0.05}$	1869^{+86}	10.19	1641	-853	-268	6
NGC 2219	06	23	44	-04	40	36	3.5	0.30	$0.8^{+0.03}$	$0.40^{+0.08}$	2023^{+93}	10.24	1660	-1118	-292	6
NGC 2220	06	21	11	-44	45	30	6.5	0.40	$3.0^{+0.12}$	$0.06^{+0.01}$	1170^{+54}	8.92	322	-1020	-475	6
NGC 2224	06	27	28	12	35	36	7.0	0.44	$0.01^{+0.00}$	$1.00^{+0.25}$	2415^{+111}	10.81	2284	-785	23	6
NGC 2234	06	29	24	16	41	00	14.0	0.84	$0.8^{+0.03}$	$0.51^{+0.10}$	1617^{+75}	10.07	1555	-434	79	6
NGC 2248	06	34	35	26	18	16	1.5	0.16	$1.0^{+0.04}$	$0.23^{+0.05}$	1740^{+80}	10.23	1707	-226	250	6
NGC 2250	06	32	48	-05	02	00	2.0	0.29	$0.6^{+0.02}$	$0.48^{+0.10}$	1795^{+83}	10.02	1456	-1031	-201	6
NGC 2260	06	38	03	-01	28	24	10.0	0.55	$0.01^{+0.00}$	$1.25^{+0.20}$	1985^{+90}	10.23	1667	-1071	-126	6
NGC 2265	06	41	41	11	54	18	6.0	0.60	$0.3^{+0.01}$	$0.48^{+0.10}$	2160^{+100}	10.54	2010	-781	123	6
NGC 2312	06	58	47	10	17	42	3.8	0.18	$0.33^{+0.01}$	$0.16^{+0.05}$	2245^{+103}	10.58	2030	-928	246	6
NGC 2318	06	59	27	-13	41	54	10.0	0.21	$0.05^{+0.00}$	$0.65^{+0.05}$	1335^{+62}	9.48	924	-958	-104	6
NGC 2331	07	06	59	27	15	42	7.0	0.04	$1.7^{+0.12}$	$0.06^{+0.02}$	1285^{+59}	9.77	1222	-210	337	6
NGC 2338	07	07	47	-05	43	12	3.5	0.21	$0.55^{+0.02}$	$0.48^{+0.05}$	1800^{+83}	9.95	1381	-1154	32	6
NGC 2348	07	03	03	-67	24	42	5.0	0.33	$1.8^{+0.07}$	$0.13^{+0.05}$	1070^{+48}	8.42	-139	-969	-432	6
NGC 2349	07	10	48	-08	35	36	9.0	0.55	$0.75^{+0.03}$	$0.61^{+0.10}$	1628^{+75}	9.76	1195	-1106	10	6

Cluster	α	δ	$R_{lim.}$	R_c	Age	E_{B-V}	R_\odot	R_{gc}	X_\odot	Y_\odot	Z	Ref.		
	h	m	s	$^\circ$	$'$	$''$	$'$	$'$	Gyr	mag	pc	kpc	pc	pc
NGC 2455	07 49 01	-21 18 06	4.0	0.24	0.18 ± 0.01	0.54 ± 0.10	2650 ± 122	10.14	1389	-2254	107	6		
NGC 2459	07 52 02	09 33 24	2.7	0.04	1.6 ± 0.11	0.03 ± 0.02	1300 ± 60	9.64	1060	-640	397	6		
NGC 2587	08 23 25	-29 30 30	2.0	0.11	0.1 ± 0.00	0.23 ± 0.10	1740 ± 80	9.26	609	-1624	136	6		
NGC 2609	08 29 32	-61 06 36	2.5	0.06	0.8 ± 0.03	0.23 ± 0.10	1320 ± 61	8.46	-138	-1280	-291	6		
NGC 2666	08 49 47	44 42 12	5.5	0.30	3.2 ± 0.13	0.03 ± 0.01	860 ± 40	9.36	664	47	544	6		
NGC 2678	08 50 02	11 20 18	6.5	0.60	2.3 ± 0.09	0.03 ± 0.01	900 ± 41	9.24	621	-452	469	6		
NGC 2932	09 35 28	-46 48 36	10.5	0.07	0.5 ± 0.02	0.55 ± 0.10	1525 ± 70	8.59	-47	-1521	103	6		
NGC 2995	09 44 04	-54 46 48	3.5	0.70	0.05 ± 0.00	1.94 ± 0.30	380 ± 17	8.46	-53	-376	-8	6		
NGC 3231	10 26 58	66 48 55	3.5	0.47	1.4 ± 0.06	0.02 ± 0.00	715 ± 33	9.07	401	314	502	6		
NGC 3446	10 52 12	-45 08 54	7.5	0.97	1.0 ± 0.04	0.16 ± 0.05	1485 ± 68	8.32	-298	-1417	329	6		
NGC 3520	11 07 08	-18 01 24	1.5	0.24	3.2 ± 0.13	0.03 ± 0.00	1245 ± 57	8.57	-13	-978	771	6		
NGC 3909	11 49 49	-48 15 06	8.0	0.99	2.0 ± 0.08	0.13 ± 0.05	1100 ± 50	8.14	-409	-989	254	6		
NGC 4230	12 17 20	-55 06 06	5.0	0.07	1.7 ± 0.12	0.23 ± 0.10	1445 ± 67	7.92	-673	-1265	187	6		
NGC 5155	13 29 35	-63 25 30	8.5	0.08	1.5 ± 0.18	0.06 ± 0.02	1070 ± 49	7.9	-647	-852	-16	6		
NGC 5269	13 44 44	-62 54 54	1.5	0.02	0.16 ± 0.11	0.52 ± 0.10	1410 ± 65	7.69	-886	-1096	-16	6		
NGC 5299	13 50 26	-59 56 54	16.5	0.29	2.0 ± 0.08	0.19 ± 0.05	1111 ± 50	7.83	-717	-847	40	6		
NGC 5381	14 00 41	-59 35 12	5.5	0.67	1.6 ± 0.11	0.06 ± 0.02	1170 ± 54	7.77	-776	-874	43	6		
NGC 5800	15 01 47	-51 55 06	6.0	0.14	0.9 ± 0.04	0.62 ± 0.10	2146 ± 99	6.92	-1692	-1301	222	6		
NGC 5925	15 27 26	-54 31 42	12.0	0.12	0.25 ± 0.01	0.58 ± 0.10	1040 ± 48	7.68	-845	-606	31	6		
NGC 5998	15 49 34	-28 35 18	4.5	0.65	2.2 ± 0.09	0.16 ± 0.05	981 ± 45	7.56	-886	-257	332	6		
NGC 6334	17 20 49	-36 06 12	15.5	0.99	0.5 ± 0.02	1.06 ± 0.25	1025 ± 47	7.49	-1013	-158	8	6		
NGC 6357	17 24 43	-34 12 06	2.5	0.20	0.4 ± 0.02	1.35 ± 0.30	1205 ± 55	7.3	-1196	-143	19	6		
NGC 6360	17 24 27	-29 52 18	2.5	0.74	0.02 ± 0.00	1.11 ± 0.20	1337 ± 62	7.17	-1333	-76	73	6		
NGC 6374	17 32 18	-32 36 00	1.8	0.15	1.3 ± 0.05	0.48 ± 0.05	900 ± 41	7.6	-897	-73	7	6		
NGC 6421	17 45 44	-33 41 36	4.0	0.12	0.17 ± 0.01	1.26 ± 0.20	1505 ± 69	7.0	-1500	-107	-63	6		
NGC 6437	17 48 24	-35 21 00	7.5	0.31	0.2 ± 0.01	0.71 ± 0.05	943 ± 43	7.56	-936	-91	-69	6		
NGC 6507	17 59 50	-17 27 00	6.6	0.45	0.40 ± 0.02	0.85 ± 0.09	1230 ± 55	7.3	-1203	246	65	1		
NGC 6525	18 02 06	11 01 24	6.5	0.88	2.0 ± 0.08	0.14 ± 0.03	1436 ± 66	7.46	-1097	838	393	6		
NGC 6573	18 13 41	-22 07 06	0.9	0.15	0.01 ± 0.00	2.48 ± 0.20	460 ± 21	8.05	-454	72	-17	6		
NGC 6588	18 20 33	-63 48 30	2.5	0.13	1.6 ± 0.11	0.10 ± 0.03	960 ± 44	7.68	-783	-437	-342	6		
NGC 6595	18 17 04	-19 51 54	2.0	0.27	0.45 ± 0.02	0.94 ± 0.10	1640 ± 76	6.90	-1607	325	-49	6		
NGC 6605	18 18 21	-14 56 42	8.5	0.46	0.6 ± 0.02	0.52 ± 0.10	889 ± 40	7.65	-855	244	5	6		
NGC 6625	18 22 50	-11 57 42	7.7	0.22	0.50 ± 0.03	1.21 ± 0.13	1335 ± 60	7.25	-1262	435	19	1		
NGC 6645	18 32 37	-16 53 00	7.4	0.79	0.40 ± 0.03	0.36 ± 0.07	1245 ± 55	7.31	-1195	338	-82	1		
NGC 6647	18 32 50	-17 13 56	6.5	0.75	1.60 ± 0.05	0.54 ± 0.10	2200 ± 100	6.4	-2119	577	-137	1		
NGC 6659	18 33 59	23 35 42	7.0	0.11	4.0 ± 0.16	0.10 ± 0.03	1155 ± 53	7.85	-682	888	282	6		
NGC 6698	18 48 04	-25 52 42	5.5	0.40	1.9 ± 0.07	0.32 ± 0.05	1150 ± 53	7.37	-1115	182	-215	6		
NGC 6724	18 56 46	10 25 42	3.0	0.13	0.9 ± 0.03	1.00 ± 0.10	1105 ± 51	7.73	-809	750	69	6		
NGC 6735	19 00 37	00 28 30	6.0	0.03	0.5 ± 0.02	0.87 ± 0.15	1466 ± 68	7.34	-1209	828	-47	6		
NGC 6737	19 02 20	-18 32 59	4.4	0.41	0.50 ± 0.02	0.76 ± 0.11	2120 ± 95	6.51	-1988	624	-392	1		
NGC 6743	19 01 20	29 16 36	3.5	0.08	1.4 ± 0.05	0.19 ± 0.05	1111 ± 51	8.01	-539	948	211	6		

Cluster	α <i>h m s</i>	δ <i>° ' "</i>	$R_{lim.}$,	R_c ,	Age <i>Gyr</i>	E_{B-V} <i>mag</i>	R_\odot <i>pc</i>	R_{gc} <i>kpc</i>	X_\odot <i>pc</i>	Y_\odot <i>pc</i>	Z <i>pc</i>	Ref.
NGC 6839	19 54 33	17 56 18	3.0	0.90	1.4 ± 0.05	0.29 ± 0.05	1410 ± 65	7.8	-783	1166	-127	6
NGC 6840	19 55 18	12 07 36	3.0	0.04	1.3 ± 0.04	0.25 ± 0.05	1970 ± 90	7.42	-1223	1518	-283	6
NGC 6843	19 56 06	12 09 48	2.5	0.26	1.3 ± 0.04	0.30 ± 0.05	1945 ± 90	7.44	-1203	1501	-284	6
NGC 6846	19 56 28	32 20 54	2.4	0.12	0.55 ± 0.02	0.68 ± 0.05	1445 ± 67	8.09	-525	1345	48	6
NGC 6847	19 56 37	30 12 48	10.0	0.74	0.5 ± 0.02	0.58 ± 0.05	1894 ± 87	7.95	-743	1742	26	6
NGC 6856	19 59 17	56 07 48	1.6	0.08	1.8 ± 0.06	0.16 ± 0.02	1704 ± 79	8.66	-9	1657	398	6
NGC 6858	20 02 56	11 15 30	5.0	0.59	2.5 ± 0.10	0.13 ± 0.02	1310 ± 60	7.75	-805	1007	-234	6
NGC 6859	20 03 49	00 26 36	5.0	0.07	3.0 ± 0.12	0.19 ± 0.05	1335 ± 62	7.56	-957	856	-364	6
NGC 6873	20 07 13	21 06 06	7.5	0.90	0.88 ± 0.04	0.35 ± 0.05	1250 ± 58	7.96	-613	1081	-134	6
NGC 6895	20 16 29	50 13 48	8.0	0.85	1.0 ± 0.04	0.35 ± 0.05	1141 ± 53	8.5	-81	1126	164	6
NGC 6904	20 21 48	25 44 24	4.0	0.69	1.0 ± 0.04	0.39 ± 0.05	1355 ± 62	8.05	-545	1232	-149	6
NGC 6938	20 34 42	22 12 54	3.6	0.29	1.3 ± 0.04	0.13 ± 0.05	1250 ± 58	8.05	-521	1112	-233	6
NGC 6950	20 41 04	16 37 06	7.5	0.41	1.8 ± 0.05	0.06 ± 0.02	1070 ± 49	8.04	-499	904	-281	6
NGC 7005	21 01 57	-12 52 50	2.0	0.22	2.5 ± 0.10	0.03 ± 0.01	1033 ± 48	7.69	-689	497	-588	6
NGC 7011	21 01 49	47 21 12	2.2	0.14	0.4 ± 0.01	1.08 ± 0.10	1236 ± 57	8.55	-40	1235	13	6
NGC 7023	21 01 35	68 10 12	7.2	0.33	0.12 ± 0.00	1.10 ± 0.10	560 ± 26	8.65	132	527	137	6
NGC 7024	21 06 09	41 29 18	2.5	0.23	0.5 ± 0.02	1.10 ± 0.10	1760 ± 81	8.51	-175	1747	-119	6
NGC 7037	21 10 54	33 45 48	3.0	0.01	2.1 ± 0.08	0.16 ± 0.05	1485 ± 68	8.35	-276	1437	-252	6
NGC 7050	21 15 12	36 10 24	3.5	0.45	2.0 ± 0.08	0.16 ± 0.05	1179 ± 54	8.41	-171	1152	-180	6
NGC 7055	21 19 30	57 34 12	2.5	0.08	0.8 ± 0.03	1.10 ± 0.10	1275 ± 59	8.76	165	1258	124	6
NGC 7071	21 26 39	47 55 12	4.0	0.15	0.3 ± 0.01	1.14 ± 0.20	1684 ± 78	8.71	42	1682	-59	6
NGC 7084	21 32 33	17 30 30	8.0	0.90	1.5 ± 0.06	0.10 ± 0.05	765 ± 35	8.27	-239	655	-315	6
NGC 7093	21 34 21	45 57 54	6.5	0.04	0.9 ± 0.04	0.61 ± 0.05	1785 ± 82	8.72	32	1780	-135	6
NGC 7127	21 43 41	54 37 48	2.5	0.15	0.4 ± 0.02	0.90 ± 0.05	1445 ± 67	8.82	199	1431	29	6
NGC 7129	21 42 59	66 06 48	3.5	0.21	0.12 ± 0.01	0.97 ± 0.05	1070 ± 49	8.84	280	1016	184	6
NGC 7134	21 48 55	-12 58 24	1.5	0.10	3.3 ± 0.13	0.06 ± 0.02	1065 ± 49	7.74	-558	502	-755	6
NGC 7175	21 58 46	54 49 06	16.0	0.18	0.25 ± 0.01	0.87 ± 0.05	1930 ± 89	9.03	326	1902	-3	6
NGC 7193	22 03 03	10 48 06	6.5	0.39	4.5 ± 0.18	0.03 ± 0.00	1080 ± 50	8.2	-304	839	-608	6
NGC 7352	22 39 43	57 23 42	4.5	0.03	0.05 ± 0.00	1.10 ± 0.20	2550 ± 117	9.52	698	2452	-47	6
NGC 7394	22 50 23	52 08 06	4.5	0.20	0.6 ± 0.02	0.35 ± 0.05	1310 ± 60	8.92	332	1259	-147	6
NGC 7429	22 56 00	59 58 24	7.0	0.06	0.04 ± 0.00	1.16 ± 0.10	1190 ± 55	8.96	387	1125	6	6
NGC 7686	23 30 07	49 08 00	8.0	0.80	2.0 ± 0.08	0.20 ± 0.05	1534 ± 71	9.13	502	1416	-307	6
NGC 7708	23 35 01	72 50 00	12.0	0.90	2.0 ± 0.08	0.42 ± 0.05	1607 ± 74	9.35	726	1401	301	6
NGC 7795	23 58 37	60 02 06	10.5	0.19	0.45 ± 0.02	1.00 ± 0.10	2105 ± 97	9.62	935	1885	-79	6
NGC 7801	00 00 21	50 44 30	4.0	0.98	1.7 ± 0.12	0.17 ± 0.05	1275 ± 60	9.11	523	1136	-250	6
NGC 7826	00 05 17	-20 41 30	10.0	0.80	2.2 ± 0.09	0.03 ± 0.01	620 ± 29	8.23	-62	117	-606	6
NGC 7833	00 06 31	27 38 30	1.3	0.10	2.0 ± 0.08	0.06 ± 0.02	1410 ± 65	9.10	416	1090	-792	6
Berkeley 1	00 09 36	60 28 30	2.5	0.14	0.4 ± 0.03	0.78 ± 0.06	2420 ± 110	9.9	1128	2139	-84	2
Berkeley 6	01 51 11	61 03 40	3.0	0.15	0.1 ± 0.00	0.78 ± 0.05	2300 ± 105	10.1	1481	1759	-38	2
Berkeley 26	06 50 18	05 45 00	2.6	0.13	0.6 ± 0.03	0.54 ± 0.05	2720 ± 120	11.0	2407	-1262	112	2
Berkeley 37	07 20 24	-01 06 00	3.5	0.69	0.9 ± 0.04	0.12 ± 0.02	4555 ± 210	12.4	3605	-2740	470	2

Cluster		α	δ	$R_{lim.}$	R_c	Age	E_{B-V}	R_\odot	R_{gc}	X_\odot	Y_\odot	Z	Re			
		h	m	s	$^\circ$	$'$	$''$	'	'	Gyr	mag	pc	kpc	pc	pc	
Berkeley	61	00	48	30	67	12	00	3.5	0.19	0.8 ± 0.05	1.09 ± 0.11	3335 ± 150	10.7	1794	2800	252
Berkeley	63	02	19	36	63	43	00	3.6	0.35	0.5 ± 0.02	0.90 ± 0.09	3305 ± 150	11.0	2231	2434	144
Berkeley	72	05	50	18	22	12	00	3.5	0.08	0.6 ± 0.02	0.79 ± 0.07	3810 ± 175	12.3	3783	-419	-171
Berkeley	76	07	06	40	-11	44	00	4.5	0.96	0.8 ± 0.04	0.73 ± 0.05	2505 ± 115	10.4	1764	-1770	-87
Berkeley	84	20	04	43	33	54	18	1.1	0.06	0.12 ± 0.01	0.76 ± 0.05	2025 ± 95	8.1	-661	1912	45
Berkeley	89	20	24	36	46	03	00	2.5	0.08	0.85 ± 0.05	1.03 ± 0.10	3005 ± 135	8.7	-357	2973	253
Berkeley	90	20	35	18	46	50	00	2.5	0.22	0.1 ± 0.01	1.15 ± 0.10	2430 ± 70	8.6	-216	2415	160
Berkeley	91	21	10	52	48	32	12	1.7	0.13	0.5 ± 0.02	1.00 ± 0.09	2400 ± 110	8.8	2.7	2400	5.5
Berkeley	95	22	28	18	59	08	00	2.4	0.29	0.15 ± 0.02	1.21 ± 0.12	1900 ± 85	9.2	507	1830	40
Berkeley	97	22	39	30	59	01	00	2.0	0.10	0.02 ± 0.00	0.75 ± 0.05	1800 ± 85	9.2	516	1724	12
Berkeley	100	23	25	58	63	46	48	2.2	0.29	0.16 ± 0.01	1.21 ± 0.11	3355 ± 155	10.3	1345	3070	144
Berkeley	101	23	32	47	64	12	30	2.2	0.23	0.7 ± 0.05	1.11 ± 0.10	2500 ± 115	9.8	1036	2272	115
Berkeley	102	23	38	42	56	38	00	3.3	0.28	0.6 ± 0.03	0.69 ± 0.05	2600 ± 120	9.8	1013	2384	-219
Berkeley	103	23	45	12	59	18	00	2.5	0.36	0.5 ± 0.02	1.00 ± 0.11	2100 ± 95	9.6	872	1908	-91
Kronberger	2	18	21	19	-14	17	12	2.5	0.08	0.10 ± 0.00	1.10 ± 0.10	3065 ± 140	5.6	-2934	887	1.5
Kronberger	3	19	39	00	06	46	00	1.0	0.03	1.60 ± 0.11	0.38 ± 0.08	1870 ± 85	7.3	-1324	1299	-240
Kronberger	5	19	46	05	27	50	00	3.5	0.08	0.16 ± 0.02	2.10 ± 0.40	615 ± 30	8.2	-273	551	17
Kronberger	12	06	14	16	22	29	52	1.4	0.17	0.16 ± 0.02	0.97 ± 0.05	1775 ± 80	10.3	1753	-271	74
Kronberger	13	19	25	15	13	56	44	1.2	0.08	0.40 ± 0.01	1.13 ± 0.11	1380 ± 65	7.7	-902	1044	-24
Kronberger	18	05	18	36	37	37	18	4.0	0.36	0.10 ± 0.00	1.29 ± 0.12	3250 ± 150	11.7	3197	584	1.9
Kronberger	23	23	05	59	60	15	14	0.9	0.15	0.10 ± 0.01	1.35 ± 0.12	1740 ± 80	9.2	601	1633	0.44
Kronberger	25	18	22	40	-14	43	41	0.8	0.10	0.05 ± 0.00	1.32 ± 0.11	1220 ± 55	7.3	-1169	348	-10
Kronberger	28	20	06	32	35	34	34	0.75	0.09	0.40 ± 0.01	2.26 ± 0.42	550 ± 25	8.4	-165	524	18
Kronberger	52	19	58	08	30	53	18	1.2	0.06	0.13 ± 0.01	2.45 ± 0.44	705 ± 30	8.3	-268	652	10.5
Kronberger	54	20	03	08	31	58	01	0.8	0.11	0.25 ± 0.02	0.94 ± 0.04	1715 ± 80	8.0	-612	1602	15.5
Kronberger	55	23	53	09	62	47	12	1.1	0.07	0.40 ± 0.02	1.13 ± 0.11	1260 ± 60	9.1	559	1129	15
Kronberger	57	20	23	58	36	36	17	2.2	0.16	0.16 ± 0.02	1.06 ± 0.09	1295 ± 60	8.3	-328	1253	-11
Kronberger	58	20	20	48	41	12	17	0.25	0.01	0.16 ± 0.02	1.35 ± 0.12	1515 ± 70	8.3	-295	1484	69.5
Kronberger	59	20	23	50	40	08	53	1.0	0.04	0.10 ± 0.00	0.84 ± 0.11	780 ± 35	8.4	-144	766	0.05
Kronberger	60	06	04	10	31	29	44	1.6	0.12	0.80 ± 0.03	0.84 ± 0.11	1960 ± 90	10.5	1953	6.6	162
Kronberger	68	20	00	36	30	35	23	2.2	0.18	0.20 ± 0.03	2.19 ± 0.40	710 ± 30	8.2	-270	567	3.1
Kronberger	72	20	12	19	37	53	27	2.0	0.23	0.50 ± 0.02	0.55 ± 0.08	1055 ± 50	8.3	-271	1019	39
Kronberger	73	20	13	47	36	44	55	1.2	0.09	0.40 ± 0.02	0.97 ± 0.05	1695 ± 80	8.2	-458	1632	37
Kronberger	74	20	17	57	36	45	37	1.1	0.05	1.00 ± 0.04	0.87 ± 0.05	1760 ± 80	8.2	-462	1698	18
Kronberger	80	21	11	50	52	22	48	1.7	0.16	0.70 ± 0.03	1.29 ± 0.10	1355 ± 60	8.7	69	1352	66
Kronberger	84	21	35	32	53	30	49	2.2	0.19	0.60 ± 0.02	0.61 ± 0.07	1075 ± 50	8.7	117	1068	21
Kronberger	85	07	58	21	-34	46	11	1.5	0.11	0.30 ± 0.01	1.00 ± 0.10	1525 ± 70	9.1	497	-1440	-76
Czernik	1	00	07	38	61	28	30	2.5	0.12	0.005 ± 0.00	1.23 ± 0.11	2530 ± 115	9.9	1177	2239	-42
Czernik	2	00	43	42	60	09	00	5.8	0.08	0.10 ± 0.01	0.74 ± 0.12	1775 ± 80	9.6	939	1504	-84
Czernik	3	01	03	06	62	47	00	2.4	0.14	0.10 ± 0.01	1.42 ± 0.14	1410 ± 65	9.4	794	1165	-1.4
Czernik	4	01	35	24	61	26	00	2.6	0.77	0.10 ± 0.01	1.06 ± 0.10	1630 ± 75	9.6	1007	1281	-28

Cluster	α	δ	$R_{lim.}$	R_c	Age	E_{B-V}	R_\odot	R_{gc}	X_\odot	Y_\odot	Z	Ref		
	h	m	s	$^\circ$	$'$	$''$	$'$	$'$	Gyr	mag	pc	kpc	pc	pc
Czernik 14	03 16 54	58 36 00	2.0	0.03	0.25 ± 0.07	1.71 ± 0.13	2175 ± 100	10.3	1688	1371	35	4		
Czernik 15	03 23 12	52 15 00	2.4	0.21	0.02 ± 0.00	1.00 ± 0.10	1155 ± 55	9.5	945	659	-80	4		
Czernik 16	03 30 48	52 39 00	5.0	0.55	0.20 ± 0.03	1.29 ± 0.10	2580 ± 120	10.7	2132	1447	-134	4		
Czernik 17	03 52 24	61 57 00	3.6	0.39	0.40 ± 0.04	0.87 ± 0.05	2120 ± 95	10.3	1673	1281	228	4		
Czernik 25	06 13 06	06 59 00	5.0	0.60	0.13 ± 0.02	0.58 ± 0.07	1980 ± 90	10.4	1824	-748	-181	4		
Czernik 26	06 30 48	-04 13 00	2.7	0.08	0.17 ± 0.02	0.45 ± 0.06	1200 ± 55	9.5	984	-673	-136	4		
Czernik 30	07 31 18	-09 58 00	3.6	0.32	0.13 ± 0.01	0.35 ± 0.04	2275 ± 105	10.2	1566	-1642	165	4		
Czernik 37	17 53 17	-27 22 10	1.8	0.10	0.60 ± 0.03	1.03 ± 0.10	1730 ± 80	6.77	-1728	67	-19	1		
Czernik 38	18 49 42	04 56 00	5.0	0.11	0.01 ± 0.00	2.03 ± 0.36	1910 ± 90	7.1	-1521	1152	88	4		
Czernik 39	19 07 44	04 20 00	2.5	0.04	0.01 ± 0.00	2.90 ± 0.45	1340 ± 60	7.5	-1046	836	-38	4		
Czernik 42	22 39 48	59 54 54	3.5	0.46	0.01 ± 0.00	1.74 ± 0.12	2585 ± 120	9.6	761	2470	52	4		
Czernik 44	23 33 30	61 57 00	4.0	0.08	0.16 ± 0.04	1.48 ± 0.10	3450 ± 160	10.4	1398	3154	27	4		
Czernik 45	23 56 18	64 33 00	2.5	0.19	0.02 ± 0.00	1.45 ± 0.11	2530 ± 115	9.9	1150	2251	102	4		
Dol-Dzim 1	02 47 30	17 16 00	7.0	0.16	5.00 ± 0.25	0.10 ± 0.03	960 ± 45	9.4	710	278	-584	4		
Dol-Dzim 2	05 23 54	11 28 00	5.0	0.38	0.80 ± 0.03	0.65 ± 0.11	1220 ± 55	9.7	1159	-251	-286	4		
Dol-Dzim 3	05 33 42	26 29 00	4.5	0.19	0.40 ± 0.02	0.77 ± 0.13	2530 ± 115	11.0	2525	-30	-156	4		
Dol-Dzim 4	05 35 54	25 57 00	12.0	0.26	0.10 ± 0.00	1.10 ± 0.18	1220 ± 55	9.7	1217	-30	-73	4		
Dol-Dzim 5	16 27 24	38 04 00	15.0	0.55	2.0 ± 0.09	0.02 ± 0.00	900 ± 40	8.1	-316	567	624	4		
Dol-Dzim 6	16 45 24	38 21 00	4.0	0.53	5.0 ± 0.26	0.03 ± 0.00	820 ± 35	8.1	-297	549	531	4		
Dol-Dzim 7	17 10 36	15 32 00	3.0	0.88	2.0 ± 0.11	0.13 ± 0.02	1140 ± 50	7.6	-802	589	555	4		
Dol-Dzim 8	17 26 12	24 11 00	8.0	0.90	3.0 ± 0.12	0.06 ± 0.00	2330 ± 100	7.1	-1392	1494	1123	4		
Dol-Dzim 9	18 08 48	31 32 00	12.0	0.30	2.3 ± 0.10	0.06 ± 0.00	2330 ± 100	7.6	-1091	1752	845	4		
Dol-Dzim 10	20 05 48	40 32 00	2.5	0.07	1.0 ± 0.05	0.55 ± 0.09	1670 ± 75	8.3	-384	1620	135	4		
Dol-Dzim 11	20 51 00	35 57 00	3.0	0.40	2.0 ± 0.11	0.42 ± 0.05	2545 ± 115	8.4	-522	2480	-232	4		
Ruprecht 13	07 08 03	-25 52 00	4.5	0.07	1.00 ± 0.05	0.26 ± 0.05	1300 ± 60	9.3	685	-1090	-185	9		
Ruprecht 15	07 19 33	-19 38 00	5.5	0.32	0.50 ± 0.03	0.65 ± 0.05	1845 ± 85	9.7	1095	-1482	-93	8		
Ruprecht 16	07 23 10	-19 28 00	3.5	0.31	0.16 ± 0.02	0.71 ± 0.07	2160 ± 100	9.9	1276	-1742	-78	9		
Ruprecht 24	07 31 54	-12 45 00	5.0	0.54	0.06 ± 0.00	0.35 ± 0.05	1983 ± 90	9.9	1300	-1492	103	9		
Ruprecht 135	17 58 12	-11 39 00	3.0	0.50	0.50 ± 0.02	1.10 ± 0.05	1850 ± 85	6.74	-1764	520	201	1		
Ruprecht 137	18 00 16	-25 13 39	2.8	0.25	0.80 ± 0.06	0.67 ± 0.05	1450 ± 65	7.06	-1445	123	-23	1		
Ruprecht 138	17 59 56	-24 40 57	3.0	0.21	2.00 ± 0.11	0.18 ± 0.05	930 ± 40	7.57	-926	86	-9	1		
Ruprecht 142	18 32 11	-12 13 47	3.3	0.03	0.40 ± 0.04	0.91 ± 0.05	1735 ± 80	6.89	-1631	590	-41	1		
Ruprecht 168	17 52 46	-28 26 00	2.6	0.80	2.00 ± 0.12	1.06 ± 0.11	820 ± 35	7.68	-820	18	-16	1		
Ruprecht 169	17 59 22	-24 46 01	2.6	0.14	1.00 ± 0.05	0.66 ± 0.05	1390 ± 60	7.12	-1384	125	-13	1		
Ruprecht 171	18 32 11	-16 02 59	5.7	0.26	3.20 ± 0.15	0.12 ± 0.03	1140 ± 50	7.41	-1092	323	-62	1		
Dolidze 9	20 25 42	41 56 00	3.0	0.72	0.02 ± 0.00	0.80 ± 0.05	866 ± 40	8.4	-152	852	35	5		
Dolidze 10	20 26 18	40 07 00	1.8	0.32	0.25 ± 0.05	0.80 ± 0.05	950 ± 44	8.4	-190	931	19	5		
Dolidze 11	20 26 30	41 27 00	2.5	0.27	0.40 ± 0.03	0.83 ± 0.06	1127 ± 52	8.4	-204	1108	37	5		
Dolidze 19	05 23 42	08 11 00	12.0	0.40	0.16 ± 0.05	0.55 ± 0.02	1320 ± 60	9.8	1229	-332	-349	5		
Dolidze 21	05 27 24	07 04 00	6.0	0.65	0.20 ± 0.08	0.55 ± 0.03	1447 ± 65	9.9	1339	-399	-377	5		
Dolidze 26	07 30 06	11 54 00	11.0	0.80	0.10 ± 0.01	0.44 ± 0.04	1907 ± 88	10.2	1657	-826	458	5		

Cluster	α <i>h m s</i>	δ <i>° ' "</i>	$R_{lim.}$,	R_c ,	Age <i>Gyr</i>	E_{B-V} <i>mag</i>	R_\odot <i>pc</i>	R_{gc} <i>kpc</i>	X_\odot <i>pc</i>	Y_\odot <i>pc</i>	Z <i>pc</i>	Ref
Dias 2	06 09 09	04 35 24	5.5	0.41	0.79 ± 0.02	0.61 ± 0.11	2835 ± 130	11.2	2570	-1142	-358	3
Dias 3	07 10 28	-08 26 14	8.0	0.88	1.41 ± 0.11	0.64 ± 0.11	4650 ± 215	12.3	3423	-3147	28	3
Dias 4	13 43 40	-63 01 30	3.2	0.04	1.26 ± 0.09	0.60 ± 0.10	2150 ± 100	7.3	-1347	-1675	-28	3
Dias 6	18 30 30	-12 18 59	3.0	0.28	0.60 ± 0.02	0.91 ± 0.07	1580 ± 70	7.03	-1488	530	-28	1
Dias 7	19 49 22	21 09 48	5.0	0.22	2.00 ± 0.10	0.42 ± 0.04	2540 ± 115	7.5	-1334	2158	-109	3
Dias 8	19 52 07	11 37 54	5.0	0.12	2.24 ± 0.10	0.30 ± 0.05	2220 ± 100	7.3	-1404	1693	-302	3
Turner 2	18 17 11	-18 49 27	3.8	0.87	0.10 ± 0.01	0.36 ± 0.04	1190 ± 55	7.34	-1163	250	-27	1
Turner 6	10 59 01	-59 29 58	1.3	0.11	0.08 ± 0.01	1.32 ± 0.13	3250 ± 145	8.0	278	-3071	18	4
Turner 7	14 32 33	-56 53 12	13.0	0.32	0.08 ± 0.01	1.39 ± 0.15	1800 ± 80	7.3	-251	-1238	104	4
Turner 8	19 45 16	27 50 30	5.0	0.34	5.00 ± 0.30	1.16 ± 0.12	2160 ± 100	7.8	-30	1933	64	4
Turner 11	20 43 24	35 35 18	8.2	0.45	0.40 ± 0.03	1.13 ± 0.10	1905 ± 85	8.3	-30	1850	-142	4
King 17	05 08 24	39 05 00	2.8	0.16	0.79 ± 0.03	0.73 ± 0.12	2960 ± 135	11.4	2887	650	-38	3
King 18	22 52 06	58 17 00	2.4	0.16	0.35 ± 0.03	0.52 ± 0.07	1860 ± 85	9.2	567	1770	-33	3
King 23	07 21 47	-00 59 06	3.6	0.37	0.89 ± 0.04	0.16 ± 0.05	3113 ± 140	11.2	2513	-1795	390	3
King 26	19 29 01	14 52 02	2.2	0.24	0.44 ± 0.02	1.27 ± 0.15	2600 ± 120	7.1	-1656	2003	-61	3
BH 47	08 42 33	-48 05 13	7.7	0.27	0.80 ± 0.05	0.73 ± 0.05	2465 ± 110	6.03	145	-2456	-154	1
BH 60	09 15 53	-50 00 38	2.1	0.09	0.40 ± 0.01	0.67 ± 0.05	1325 ± 60	7.17	-38	-1324	-16	1
BH 218	17 16 12	-39 24 04	2.8	0.06	0.40 ± 0.01	0.88 ± 0.06	1215 ± 55	7.28	-1188	-254	-14	1
ESO 524-01	18 56 37	-26 57 39	3.0	0.30	3.20 ± 0.14	0.30 ± 0.03	2800 ± 130	5.75	-2694	430	-629	1
ESO 522-05	18 12 53	-24 21 50	2.2	0.23	3.20 ± 0.14	1.82 ± 0.15	660 ± 30	7.84	-654	80	-35	1
ESO 525-08	19 27 16	-23 34 35	3.0	0.26	1.00 ± 0.05	0.36 ± 0.04	1640 ± 75	6.93	-1505	407	-507	1
IC 1434	22 10 34	52 49 40	3.5	0.27	0.32 ± 0.02	0.66 ± 0.05	3035 ± 140	9.5	523	2986	-143	3
IC 2156	06 04 51	24 09 30	2.0	0.07	0.25 ± 0.02	0.67 ± 0.05	2100 ± 95	10.6	2087	-230	47	3
IC 4291	13 36 56	-62 05 45	2.8	0.09	0.80 ± 0.04	0.61 ± 0.05	1790 ± 82	7.53	-1107	-1406	10	1
Alessi 15	06 43 04	01 40 19	6.0	0.12	0.45 ± 0.03	0.91 ± 0.07	2509 ± 116	10.74	2161	-1273	-48	7
Alessi 53	06 29 24	09 10 39	6.4	0.13	0.50 ± 0.04	0.61 ± 0.05	2360 ± 109	10.72	2184	-894	-27	7
Juchert 1	19 22 32	12 40 00	1.6	0.04	0.40 ± 0.03	1.36 ± 0.10	2286 ± 105	7.16	-1538	1691	-40	7
Juchert 12	07 20 57	-22 52 00	5.0	0.36	0.30 ± 0.02	0.91 ± 0.07	3016 ± 139	10.47	1658	-2510	-217	7
Riddle 4	02 07 23	60 15 25	2.2	0.13	0.05 ± 0.05	0.91 ± 0.07	1993 ± 92	9.95	1339	1475	-43	7
Riddle 15	19 11 09	14 50 04	2.5	0.08	0.50 ± 0.03	1.33 ± 0.10	1925 ± 89	7.36	-1278	1437	82	7
Skiff 1	06 14 47	12 52 15	1.5	0.10	0.25 ± 0.01	0.57 ± 0.04	3150 ± 145	5.35	3005	-937	-115	1
Skiff 2	04 58 14	43 00 48	2.5	0.30	0.90 ± 0.06	0.18 ± 0.05	2125 ± 100	6.37	2032	621	5	1
Teutsch 11	06 25 24	13 51 59	3.0	0.26	0.50 ± 0.04	0.70 ± 0.05	3443 ± 159	11.83	3280	-1044	39	7
Teutsch 144	21 21 44	50 36 36	5.0	0.30	0.80 ± 0.08	0.73 ± 0.05	1704 ± 79	8.75	81	1702	14	7
Collinder 351	17 49 00	-28 44 09	4.2	0.19	0.16 ± 0.02	0.70 ± 0.05	1310 ± 60	7.19	-1310	14	-16	1
Patchick 89	19 59 33	49 18 45	3.5	0.07	1.60 ± 0.13	0.21 ± 0.02	2646 ± 122	8.62	-288	2588	465	7
Toeppler 1	20 01 18	33 36 54	4.0	0.10	0.40 ± 0.03	0.79 ± 0.05	2890 ± 133	8.00	-974	2719	87	7

Table 2: References of studied clusters.

Number	Reference
1	Tadross, A. L., 2008, New Astronomy 13, 370.
2	Tadross, A. L., 2008, Monthly Notices of the Royal Astronomical Society 389, 285.
3	Tadross, A. L., 2009, New Astronomy 14, 200.
4	Tadross, A. L., 2009, <i>Astrophys & Space Sci.</i> 323, 383.
5	Tadross, A. L. & Nasser, M. A., 2010, NRIAG Journal Ser.”A67” (arXiv:1011.2934).
6	Tadross, A. L., 2011, Journal of the Korean Astronomical Society 44 (1), 1.
7	Tadross, A. L., et al, 2012, Research in Astronomy and Astrophysics (RAA) 12, 75.
8	Tadross, A. L., 2012, Research in Astronomy and Astrophysics (RAA) 12, 158.
9	Tadross, A. L., 2012, New Astronomy 17, 198.